



## Scientific-Research Article

# Numerical Study of Flow Visualization and Thermal Performance for Pulsating Heat Pipes

Sam M. Pouryoussefi <sup>1\*</sup>, Sohrab G. Pouryoussefi <sup>2</sup>

1- University of Missouri, Columbia, MO 65211, USA

2-Faculty of Aerospace Engineering, K. N. Toosi University of Technology

## ABSTRACT

**Keywords:** Pulsating Heat Pipe, Numerical Simulation, Thermal Performance, CFD Video Technique, Flow Visualization

*Due to the importance of pulsating heat pipes (PHPs) behavior and limitations in conducting experimental studies, numerical simulations are getting more attention. The present work uses numerical simulations for pulsating heat pipes and investigates the thermal performance of closed-loop pulsating heat pipes at different operating conditions, such as evaporator heating power and filling ratio. To this end, water, ethanol, methanol, and acetone are employed as working fluids. A two-dimensional single-loop PHP is used for the present study. Also, the computational Fluid Dynamics (CFD) video technique is employed for flow visualization purposes. Accordingly, a perfect match was observed between the present CFD video clip and previous experimental video-based studies regarding flow patterns and behavior. Moreover, the present study shows how researchers can benefit from developing numerical tools to test pulsating heat pipes' behavior at different operating conditions or working fluids without facing the difficulties and limitations of applying laboratory thermal measurement equipment or high-speed cameras. Numerical simulations show that the CFD video clip is very informative for flow visualization. Besides, the simulated clip made capturing phenomena occurring in a pulsating heat pipe much easier. Likewise, the thermal performance investigations at different operating conditions and working fluids were found to be very informative in terms of application and design purposes, especially for experimental studies. By increasing heating power greater than 60 W, circulation velocity was increased for most cases. It should be noted that phase contour videos are inserted at the bottom of the article.*

## Introduction

Conventional heat transfer mechanisms utilized for cooling/heating applications in different

1. Assistant Professor (Corresponding author) **Email:** pouryoussefis@missouri.edu

2. Assistant Professor

industries always need external power and run at some operating cost in addition to the initial manufacturing cost. Meanwhile, a heat pipe represents a solution by which large amounts of heat can be transferred with a small temperature difference between the corresponding hot and cool sources without needing any external power. Heat pipes are produced from different materials with different sizes and forms and are lighter than other heat transfer devices. In recent decades, the design of heat pipes has evolved due to continuous demand for fast small-scale microelectronic systems [1]. The oscillating or pulsating heat pipe (OPH or PHP) is a very promising heat transfer device. In addition to its excellent heat transfer performance, it has a simple structure. Unlike conventional heat pipes, there is no wick structure to return the condensed working fluid to the evaporator section. Besides, the PHP is made from a long, continuous capillary tube bent into many turns. The diameter of the PHP must be sufficiently small so that vapor plugs can be formed by capillary action. Due to the pulsation of the working fluid in the axial direction of the tube, heat is transported from the evaporator section to the condenser section. The heat input, which is the driving force, increases the pressure of the vapor plug in the evaporator section. In turn, this pressure increase will push the neighboring vapor plugs and liquid slugs toward the condenser at a lower pressure [2]. Zhang and Faghri [3], [4], [5] investigated the heat transfer process in the evaporator and condenser sections of the PHP. They developed heat transfer models in a pulsating heat pipe's evaporator and condenser sections with one open end by analyzing thin film evaporation and condensation. The results of their study showed that the frequency and amplitude of the oscillation are almost unaffected by the surface tension after steady oscillation has been established. Further, the amplitude of oscillation was decreased with decreasing diameter of the pulsating heat pipe and decreasing wall temperature of the heating section. However, the frequency of oscillation was almost unchanged. Ma et al. [6] developed A mathematical model predicting the fluid motion and temperature drop in an OHP. The model included the forced convection heat transfer due to the oscillating motions, the confined evaporating heat transfer in the evaporating section, and thin film condensation heat transfer in the condensing section. Qu et al. [7] conducted an experimental study on the

thermal performance of a silicon-based micro-PHP. The effects of gravity, filling ratio, and working fluids on the overall thermal resistance were discussed. The experimental results showed that a micro-PHP embedded in a semiconductor chip could significantly decrease the maximum localized temperature [8]. Xian et al. [9] experimentally investigated dynamic fluid flow in OHP under pulse heating. They employed a high-speed camera to conduct experiments and fluid flow visualization in PHP. Jiaqiang et al. [10] studied a closed OHP's pressure distribution and flow characteristics under different operating conditions. They analyzed the relationship between flow pattern distribution and pressure distribution. Song and Xu [11] have run a series of experiments to explore the chaotic behavior of PHPs. This study used FC-72 and de-ionized water as the working fluids. Also, A high-speed data acquisition system was used to record time series of temperatures at different locations on the PHP. FC-72 PHPs have a complex relationship between correlation dimensions and the number of turns. the results showed that correlation dimensions were increased by increasing the number of turns for water PHPs. Turkyilmazoglu investigated the effects of nanofluids on heat transfer enhancement in single- and multi-phase flows [12,13]. It was shown that by increasing the diffusion parameter in the multi-phase model, more enhancements in the rate of heat transfer could be obtained. In addition, a rescaling method was proposed to simplify the evaluation of flow and physical parameters, such as skin friction and heat transfer rate in single-phase nanofluids. Dobson [14] theoretically and experimentally investigated an open oscillatory heat pipe, including gravity. Interestingly, the theoretical model did not include convective heat transfer to and from the vapor bubble and the liquid plug. Also, in this study, an open oscillatory heat pipe was manufactured for the experiment. It was found that the theoretical model was able to reflect the characteristic chaotic behavior of the experimental devices. Xiao-Ping and Cui [15] studied the dynamic properties of the microchannel phase change in a heat transfer system by theoretical method combined with experiment. To this end, a dynamic model for a microchannel phase change in a heat transfer system has been established by considering disjoining pressure at the liquid-vapor interface due to the small size of the channel. PSD analysis showed that the system is in a state of chaos. They

concluded that the chaos of the system is one of the important conditions that lead to high heat transfer performance for microchannel systems by considering the correspondence of chaos with turbulence. Ridouane et al. [16] computationally explored the chaotic flow in a 2D natural convection loop. They set constant temperatures for the boundary conditions in the heating and cooling sections. Accordingly, numerical simulations were applied for water corresponding to the Prandtl number of 5.83 and Rayleigh number varying from 1000 to 150,000. Results were presented for each flow regime regarding streamlines, isotherms, and local heat flux distributions along the walls. Zufar et al. [17] investigated hybrid nanofluids on pulsating heat pipes numerically and experimentally. As a result, adding hybrid nanoparticles in water improved the thermal resistance of PHP. Therefore, the heating power required for start-up pulsations was lower for hybrid nanofluids.

Pouryoussefi and Zhang [18-20] conducted a numerical simulation of the chaotic flow in the closed-loop PHPs. They applied simple two-dimensional, multi-turn two-dimensional, and three-dimensional structures for the heat pipes geometry. Constant temperature and heat flux have been employed to investigate thermal performance, such as thermal resistance and axial mean temperature for several boundary conditions. Also, the volume of Fluid (VoF) method was used for liquid-vapor two-phase flow simulation. Besides, water and ethanol were used as working fluids in the pulsating heat pipe. To this end, Quantitative approaches were employed to investigate chaos in PHPs, such as spectral analysis of time series, correlation dimension, autocorrelation function (ACF), Lyapunov exponent, and phase space reconstruction.

The present study shows how researchers can benefit from developing numerical tools to test pulsating heat pipes' behavior at different operating conditions or working fluids without facing the difficulties and limitations of applying laboratory thermal measurement equipment or high-speed cameras. Expensive laboratory equipment and applying accurate operating conditions in an experiment are among the limitations of these types of studies. For instance, it is almost impossible to create an ideal adiabatic section for a pulsating heat pipe using insulators in an experiment.

The present study employed a two-dimensional single-loop PHP to conduct numerical simulations. The simple geometry of the test case made it easier to run several simulations in terms of operating conditions and working fluids. The thermal performance of closed-loop pulsating heat pipes is investigated at different operating conditions, such as evaporator heating power and filling ratio. Correspondingly, water, ethanol, methanol, and acetone are employed as working fluids. Also, the CFD video technique is employed for flow visualization purposes. The study results showed a perfect match between the present CFD video clip and previous experimental video-based studies in terms of flow patterns and behavior [21]. Two CFD video files are inserted at the bottom of the article as a result of numerical simulations. Numerical simulation showed that the CFD video clips are very informative for flow visualization purposes. Therefore, the simulated clip made capturing phenomena occurring in a pulsating heat pipe much easier. Besides, the thermal performance investigation at different operating conditions and working fluids was very informative in terms of application and design purposes, especially for experimental studies. Further research should be conducted on a comprehensive investigation using the employed CFD video technique to capture and analyze phenomena that occur in a pulsating heat pipe for their future work, such as flow motion frequency analysis. More details of the numerical simulation method and its validation can be found in the references [18-20].

### Physical modeling

Figure 1 shows the schematic view of the 2D PHP. The thickness of the pipe is 3 mm. The evaporator, adiabatic, and condenser sections are at the pulsating heat pipe's bottom, middle, and top. Water and ethanol were used as working fluids. Different evaporator heating powers and filling ratios were tested for the numerical simulation. In addition, Figure 1 shows the quadrilateral profile of the meshing configuration used in the numerical simulation. The results show that surface tension is an important factor in the performance of the pulsating heat pipe. Also, it was found that employing quadrilaterals meshes for numerical simulation leads to more accurate results in the case of surface tension than those of triangular and tetrahedral [18]. Likewise, the volume of Fluid

(VOF) method has been applied for two-phase flow simulation. The volume of fluid method is a free-surface modeling technique, i.e., a numerical technique for tracking and locating the free surface (or fluid-fluid interface). It belongs to the class of Eulerian methods, characterized by a mesh that is either stationary or moving in a specific prescribed manner to accommodate the evolving shape of the interface [20].

The criteria for grid independency were selected as the volume fraction of liquid and vapor and the flow pattern in the pipe as a function of time. The results show that no change in volume fraction and flow pattern was observed as a function of time after increasing the number of grids greater than the optimum number.

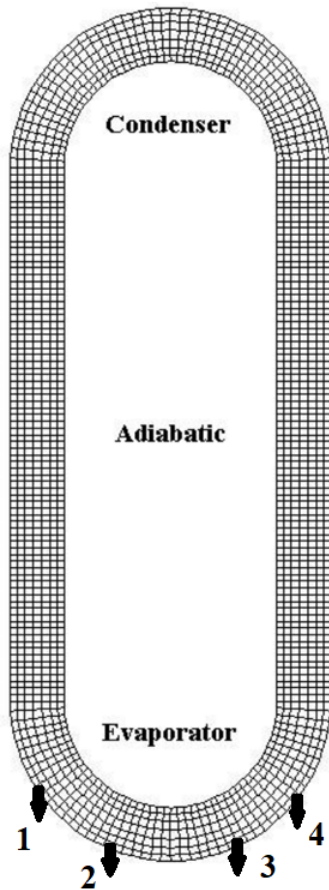


Figure 1. Meshing Configuration of the PHP (not in scale)

Tracking the interfaces between the phases is accomplished by solving a continuity equation for the volume fraction of one (or more) of the phases. For the  $q^{th}$  phase, this equation has the following form [20]:

$$\frac{1}{\rho_q} \left[ \frac{\partial}{\partial t} (\alpha_q \rho_q) + \nabla \cdot (\alpha_q \rho_q \mathbf{v}) \right] = \sum_{p=1}^n (\dot{m}_{pq} - \dot{m}_{qp}) \quad (1)$$

Where  $\dot{m}_{qp}$  is the mass transfer from phase  $q$  to phase  $p$ , and  $\dot{m}_{pq}$  is the mass transfer from phase  $p$  to phase  $q$  due to phase change. The primary-phase volume fraction will be computed based on the following constraint:

$$\sum_{q=1}^n \alpha_q = 1 \quad (2)$$

The volume fraction equation was solved using explicit time discretization. In the explicit approach, the finite-difference interpolation schemes are applied to the volume fractions that were computed in the previous time step [20]:

$$\frac{\alpha_q^{n+1} \rho_q^{n+1} - \alpha_q^n \rho_q^n}{\Delta t} V + \sum_f (\rho_q U_f^n \alpha_{q,f}^n) = \left[ \sum_{p=1}^n (\dot{m}_{pq} - \dot{m}_{qp}) + S_{\alpha_q} \right] V \quad (3)$$

Where  $n+1$  is the index for new (current) time step,  $n$  is the index for previous time step,  $\alpha_{q,f}$  is the face value of the  $q^{th}$  volume fraction,  $V$  is the volume of cell, and  $U_f$  is the volume flux through the face, based on normal velocity.

The presence of the component phases in each control volume determines the properties appearing in the transport equations. In the vapor-liquid two-phase system, the density  $\rho$  and viscosity  $\mu$  in each cell are given by [20]:

$$\rho = \alpha_v \rho_v + (1 - \alpha_v) \rho_l \quad (4)$$

$$\mu = \alpha_v \mu_v + (1 - \alpha_v) \mu_l \quad (5)$$

A single momentum equation is solved throughout the domain, and the resulting velocity field is shared among all phases. The momentum

equation, shown below, is dependent on the volume fractions of all phases through the properties  $\rho$  and  $\mu$  [20]:

$$\begin{aligned} \frac{\partial}{\partial t}(\rho \vec{v}) + \nabla \cdot (\rho \mathbf{v}\mathbf{v}) & \quad (6) \\ & = -\nabla p + \nabla \\ & \cdot [\mu(\nabla \mathbf{v} + \nabla \mathbf{v}^T)] + \rho \mathbf{g} \\ & + \mathbf{F} \end{aligned}$$

Where  $\mathbf{F}$  is the body force,  $\mathbf{g}$  is the gravity acceleration and  $\mu$  is the dynamic viscosity. One limitation of the shared-fields approximation is that in cases where large velocity differences exist between the phases, the accuracy of the velocities computed near the interface can be adversely affected.

The energy equation, also shared among the phases, is [20]:

$$\begin{aligned} \frac{\partial}{\partial t}(\rho E) + \nabla \cdot (\mathbf{v}(\rho E + p)) & \quad (7) \\ & = \nabla \cdot (k_{eff} \nabla T) + S_h \end{aligned}$$

The VOF model treats energy,  $E$ , and temperature,  $T$ , as mass-averaged variables [20]:

$$E = \frac{\sum_{q=1}^n \alpha_q \rho_q E_q}{\sum_{q=1}^n \alpha_q \rho_q} \quad (8)$$

Where  $E_q$  for each phase is based on the specific heat of that phase and the shared temperature. The properties  $\rho$  and  $k_{eff}$  (effective thermal conductivity) are shared by the phases and the source term,  $S_h$  is equal to zero.

The surface curvature is computed from local gradients in the surface normal at the interface. The surface normal  $\mathbf{n}$ , defined as the gradient of  $\alpha_q$ , the volume fraction of the  $q^{th}$  phase is [20]:

$$\mathbf{n} = \nabla \alpha_q \quad (9)$$

The curvature,  $\mathbf{K}$ , is defined in terms of the divergence of the unit normal,  $\hat{\mathbf{n}}$ :

$$\mathbf{K} = \nabla \cdot \hat{\mathbf{n}} \quad (10)$$

Where

$$\hat{\mathbf{n}} = \frac{\mathbf{n}}{|\mathbf{n}|} \quad (11)$$

is the unit surface normal vector. The surface tension can be written in terms of the pressure jump across the surface. The force at the surface can be expressed as a volume force using the divergence theorem. It is this volume force that is

the source term which is added to the momentum equation. It has the following form [20]:

$$F_{vol} = \sigma_{12} \frac{\rho k_1 \nabla \alpha_2}{\frac{1}{2}(\rho_1 + \rho_2)} \quad (12)$$

Where  $\rho$  is the volume-averaged density computed using Equation (4) and  $\sigma_{12}$  is the surface tension. Equation (12) shows that the surface tension source term for a cell is proportional to the average density in the cell.

To model the wall adhesion angle in conjunction with the surface tension model, the contact angle that the fluid is assumed to make with the wall is used to adjust the surface normal in cells near the wall. This so-called dynamic boundary condition results in the adjustment of the curvature of the surface near the wall. If  $\theta_w$  is the contact angle at the wall, then the surface normal at the live cell next to the wall is [20]:

$$\hat{\mathbf{n}} = \hat{\mathbf{n}}_w \cos \theta_w + \hat{\mathbf{t}}_w \sin \theta_w \quad (13)$$

Where  $\hat{\mathbf{n}}_w$  and  $\hat{\mathbf{t}}_w$  are the unit vectors normal and tangential to the wall, respectively. More details of numerical simulation method and its validation can be found in references [18-20].

## Results and Discussions

In addition to the investigation of thermal performance, the CFD video technique is employed for flow visualization in the pulsating heat pipe. Numerical simulations show that two CFD video files are attached to the bottom of the article. The operating conditions for the video clips are 40 and 60 W heating power, 20 °C condenser temperature, 30% filling ratio, and water and ethanol as working fluids. The CFD video files were found very interesting and informative for the flow visualization purpose. A perfect match was observed between the attached CFD video clips and other experimental video-based studies concerning flow patterns and behavior [21].

Figures 2(a) and 2(b) show two snapshots of the video clip, namely one at the initial condition and the other after the flow circulation is established at 60 W heating power and ethanol as a working fluid.

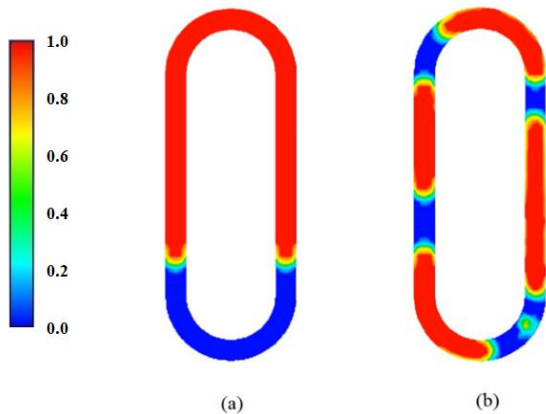


**Figure 2.** Volume fractions of liquid and vapor at initial condition (a) and after flow circulation is established (b), 60 W heating power, 20 °C condenser temperature, 30% filling ratio and ethanol as working fluid

Small bubbles, the results of the nucleate pool boiling in the evaporator section, rise in the adiabatic section of the tubes. Depending on the bubble-raised velocity, relative movement of the bulk fluid, the geometry of the heat pipe, and local heat transfer characteristics, these bubbles may reach the condenser section with reduced sizes or completely collapse due to condensation while in transit. Further, smaller bubbles usually merge with larger ones if encountered on the way. Therefore, a part of an expanding bubble breaks away from it and travels further to merge with another bubble encountered on the way. A large bubble shrinks due to condensation and may sometimes become smaller than the tube diameter and immediately floats up due to buoyancy. Hence, two or more large expanding bubbles usually coalesce to form larger bubbles that, in turn, may get subdivided again into smaller components.

Flow visualizations also indicated that there are alternating periods in which plugs/bubbles were racing (activity phase) and tending to stop for a while (static phase) [21].

The thermal resistance is an important parameter indicating the thermal performance of a pulsating heat pipe. Specifically, the overall thermal resistance of a PHP is defined as the difference in average temperatures between the evaporator and condenser divided by the heating power. As shown in Figure 1, four points are set to find the mean temperature of the evaporator section during simulations. Hence, Equation (14) was used to calculate the mean temperature of the evaporator.

$$T_{e-mean} = \frac{T_{e1} + T_{e2} + T_{e3} + T_{e4}}{4} \quad (14)$$

The mean temperature for each point is defined as the average temperature on that point after flow circulation is established.

The entire condenser section for all simulations has the same temperature due to the constant temperature boundary condition of 20 °C. Equation (15) was used to calculate the PHP's thermal resistance as a measure of thermal performance:

$$R = \frac{T_e - T_c}{Q} \quad (15)$$

Where  $T_e$  is the average temperature of evaporator,  $T_c$  is the temperature of condenser section and  $Q$  is the heating power at evaporator.

Each type of working fluid affects the thermal resistance by its thermodynamic properties, including boiling point, latent heat of vaporization, specific heat, surface tension, viscosity, and thermal conductivity. Because of the complicated and chaotic behavior of pulsating heat pipes, conducting experiments and running simulations are critical in finding out how each working fluid affects the thermal resistance.

The effects of working fluids on the thermal resistance of PHP at various heating powers and filling ratios are shown in Figures 3, 4, and 5. Obviously, there is a trend of decreasing thermal resistance with increased heating power, especially in lower values of heating power for all working fluids. Thermal resistance then behaves almost steadily afterward by increasing the heating power.

For all filling ratios, the PHP with water as a working fluid has greater thermal resistance compared to other working fluids at low heating power because of the high latent heat of vaporization. Thus, more heating power is needed to form flow circulation. For heating power up to 40 W, a long period of flow oscillations was observed before starting flow circulation. From 40 W to 60 W, oscillation periods got shorter by increasing heating power, and flow circulations started faster. In addition, the thermal resistance drop rate is lower at a filling ratio of 60% compared to 30% and 45% for water as a working fluid. By increasing heating power greater than 60 W, circulation velocity was increased for most cases. Then, thermal resistance drops were the result of such velocity increment. Nevertheless,

due to changes in flow patterns in a high range of heating powers, an increase in thermal resistance was also observed. These drops and increments are more sensible at a filling ratio of 30% in this range of heating power for water as a working fluid. Besides, thermal resistance is almost steady for 60 W to 100 W heating power for the filling ratio of 45% and 60%. Furthermore, similar behavior to water was observed for ethanol and methanol as working fluids. Flow circulations start at lower heating power for ethanol and methanol compared to water due to lower latent heat of vaporization. Thermal resistance variation for acetone as a working fluid was found to be more chaotic. A significant change in thermal resistance behavior was observed by changing the filling ratio from 30% to 45% and 60% for acetone. Unlike other working fluids, thermal resistance increases by increasing heating power at a filling ratio of 45%, except for 10W to 20W heating power. As mentioned earlier, circulation velocity and flow pattern were crucial factors affecting the thermal behavior of pulsating heat pipes, especially at a higher range of heating power for all working fluids and filling ratios. This high-temperature operating condition may lead to better thermal performance depending on other factors such as PHP's structure, working fluid, filling ratio, and condenser temperature. In addition, thermal resistance for all filling ratios and working fluids was closer in value at 60 W to 100 W heating power.

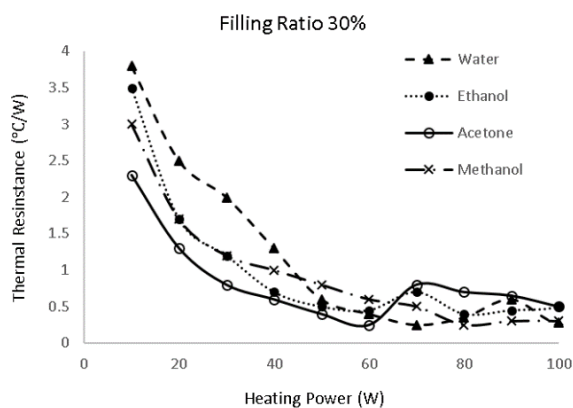


Figure 3. Thermal resistance versus heating power at a filling ratio of 30%

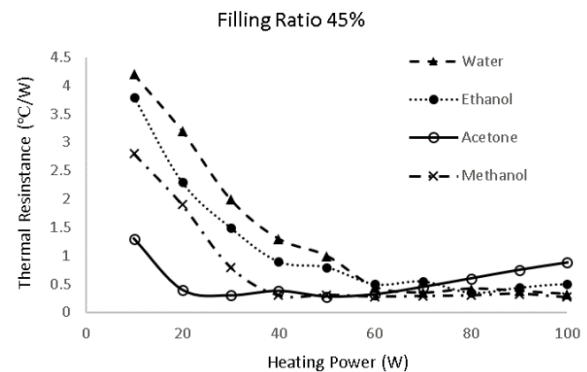


Figure 4. Thermal resistance versus heating power at a filling ratio of 45%

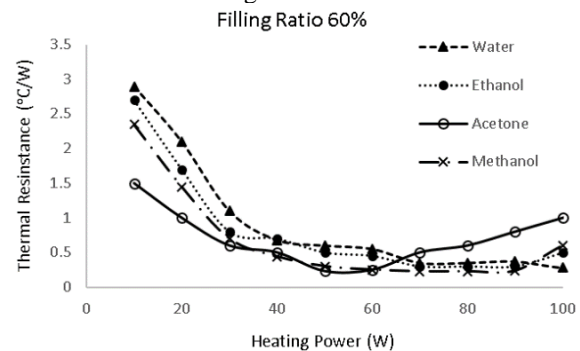


Figure 5. Thermal resistance versus heating power at a filling ratio of 60%

## Conclusions

The present study shows how researchers can benefit from developing numerical tools to test pulsating heat pipes' behavior at different operating conditions or working fluids without facing the difficulties and limitations of applying laboratory thermal measurement equipment or high-speed cameras. A two-dimensional single-loop PHP was employed to conduct numerical simulations in the current work. To this end, the thermal performance of closed-loop pulsating heat pipes was investigated at different operating conditions, such as evaporator heating power and filling ratio. Water, ethanol, methanol, and acetone were employed as working fluids. For heating power up to 40 W, a long period of flow oscillations was observed before starting flow circulation for water as a working fluid. By increasing heating power greater than 60 W, circulation velocity was increased for most cases. Then, thermal resistance drops were a result of such velocity increment. Also, flow circulations start at lower heating power for ethanol and methanol compared to water due to lower latent heat of vaporization. Accordingly, flow circulation velocity and flow pattern were found to be key

factors to affect the thermal behavior of pulsating heat pipes, especially at the higher range of heating power. Unlike other working fluids, thermal resistance increased by increasing heating power at a filling ratio of 45%, except for 10W to 20W heating power for acetone as a working fluid. Also, thermal resistance for all filling ratios and working fluids was closer in value at a range of 60 W to 100 W heating power. Thermal resistance variation for acetone as a working fluid was found to be more chaotic. Besides, the thermal performance investigations at different operating conditions and working fluids were found to be very informative in terms of application and design purposes, especially for experimental studies.

CFD video technique was employed for flow visualization purposes. Subsequently, a perfect match was observed between the present CFD video clip and previous experimental video-based studies concerning flow patterns and behavior [21]. Also, two CFD video files are attached to the bottom of the article based on numerical simulation. According to numerical simulations, the CFD video clips were found to be very informative for flow visualization purposes. The simulated clips made capturing phenomena occurring in a pulsating heat pipe much easier.

A comprehensive investigation is suggested for further research using the CFD video technique to capture and analyze phenomena that occur in a pulsating heat pipe.

## References

- [1] Mohammadi, O., Shafii, M.B., Rezaee Shirin-Abadi, A., Heydarian, R., Ahmadi, M.H.: The impacts of utilizing nano-encapsulated PCM along with RGO nanosheets in a pulsating heat pipe, a comparative study. *Int. J. Energy Res.* **45** (13), 19481-19499 (2021)
- [2] Shafii, M.B., Faghri, A., Zhang, Y.: Thermal modeling of unlooped and looped pulsating heat pipes. *J. Heat Transf.* **123** (6), 1159-1172 (2001)
- [3] Zhang, Y., Faghri, A.: Heat transfer in a pulsating heat pipe with open end. *Int. J. Heat Mass Transf.* **45** (4), 755-764 (2002)
- [4] Zhang, Y., Faghri, A.: Oscillatory flow in pulsating heat pipes with arbitrary numbers of turns. *J. Thermophys. Heat Transf.* **17** (3), 340-347 (2003)
- [5] Zhang, Y., Faghri, A.: Advances and unsolved issues in pulsating heat pipes. *Heat Transf. Eng.* **29** (1), 20-44 (2008)
- [6] Ma, H.B., Borgmeyer, B., Cheng, P., Zhang, Y.: Heat transport capability in an oscillating heat pipe. *J. Heat Transf.* **130** (8), 081501 (2008)
- [7] Qu, J., Wu, H., Cheng, P.: Experimental study on thermal performance of a silicon-based micro pulsating heat pipe. In *ASME Second International Conference on Micro/Nanoscale Heat and Mass Transfer* **43918**, 629-634 (2009)
- [8] Qu, J., Wu, H.Y., Wang, Q.: Experimental investigation of silicon-based micro-pulsating heat pipe for cooling electronics. *Nanoscale Microscale Thermophys. Eng.* **16** (1), 37-49 (2012)
- [9] Xian, H., Xu, W., Zhang, Y., Du, X., Yang, Y.: Experimental investigations of dynamic fluid flow in oscillating heat pipe under pulse heating. *Appl. Therm. Eng.* **88**, 376-383 (2015)
- [10] Jiaqiang, E., Zhao, X., Deng, Y., Zhu, H.: Pressure distribution and flow characteristics of closed oscillating heat pipe during the starting process at different vacuum degrees. *Appl. Therm. Eng.* **93**, 166-173 (2016)
- [11] Song, Y., Xu, J.: Chaotic behavior of pulsating heat pipes. *Int. J. Heat Mass Transf.* **52**(13-14), 2932-2941 (2009)
- [12] Turkyilmazoglu, M.: Anomalous heat transfer enhancement by slip due to nanofluids in circular concentric pipes. *Int. J. Heat Mass Transf.* **85**, 609-614 (2015)
- [13] Turkyilmazoglu, M.: Analytical solutions of single and multi-phase models for the condensation of nanofluid film flow and heat transfer. *Eur. J. Mech. B/Fluids* **53**, 272-277 (2015)
- [14] Dobson, R.T.: Theoretical and experimental modelling of an open oscillatory heat pipe including gravity. *Int. J. Therm. Sci.* **43** (2), 113-119 (2004)
- [15] Xiao-Ping, L., Cui, F.Z.: Modelling of phase change heat transfer system for micro-channel and chaos simulation. *Chinese Phys. Lett.* **25** (6), 2111 (2008)
- [16] Ridouane, E.H., Danforth, C.M., Hitt, D.L.: A 2-D numerical study of chaotic flow in a natural convection loop. *Int. J. Heat Mass Transf.* **53** (1-3), 76-84 (2010)
- [17] Zufar, M., Gunnasegaran, P., Kumar, H.M., Ng, K.C.: Numerical and experimental investigations of hybrid nanofluids on pulsating heat pipe performance. *Int. J. Heat Mass Transf.* **146**, 118887 (2020)
- [18] Pouryoussefi, S.M., Zhang, Y.: Numerical investigation of chaotic flow in a 2D closed-loop pulsating heat pipe. *Appl. Therm. Eng.* **98**, 617-627 (2016)
- [19] Pouryoussefi, S.M., Zhang, Y.: Analysis of chaotic flow in a 2D multi-turn closed-loop pulsating heat pipe. *Appl. Therm. Eng.* **126**, 1069-1076 (2017)
- [20] Pouryoussefi, S.M., Zhang, Y.: Nonlinear analysis of chaotic flow in a three-dimensional closed-loop pulsating heat pipe. *J. Heat Transf.* **138** (12), 122003 (2016)
- [21] Khandekar, S., Groll, M., Charoensawan, P., Terdtoon, P.: Pulsating heat pipes: thermo-fluidic characteristics and comparative study with single phase thermosyphon. In *International Heat Transfer Conference Digital Library*, Begel House Inc. (2002).

## COPYRIGHTS

©2022 by the authors. Published by Iranian Aerospace Society This article is an open access article distributed under the terms and conditions of the Creative Commons Attribution 4.0 International (CC BY 4.0) (<https://creativecommons.org/licenses/by/4.0/>).

